Brain PPARγ Promotes Obesity and is Required for the Insulin–Sensitizing Effect of Thiazolidinediones

Authors: Min Lu, David A. Sarruf, Saswata Talukdar, Shweta Sharma, Pingping Li, Gautam Bandyopadhyay, Sarah Nalbandian, WuQiang Fan, Jiaur R. Gayen, Sushil K. Mahata, Nicholas J. Webster, Michael W. Schwartz, and Jerrold M. Olefsky

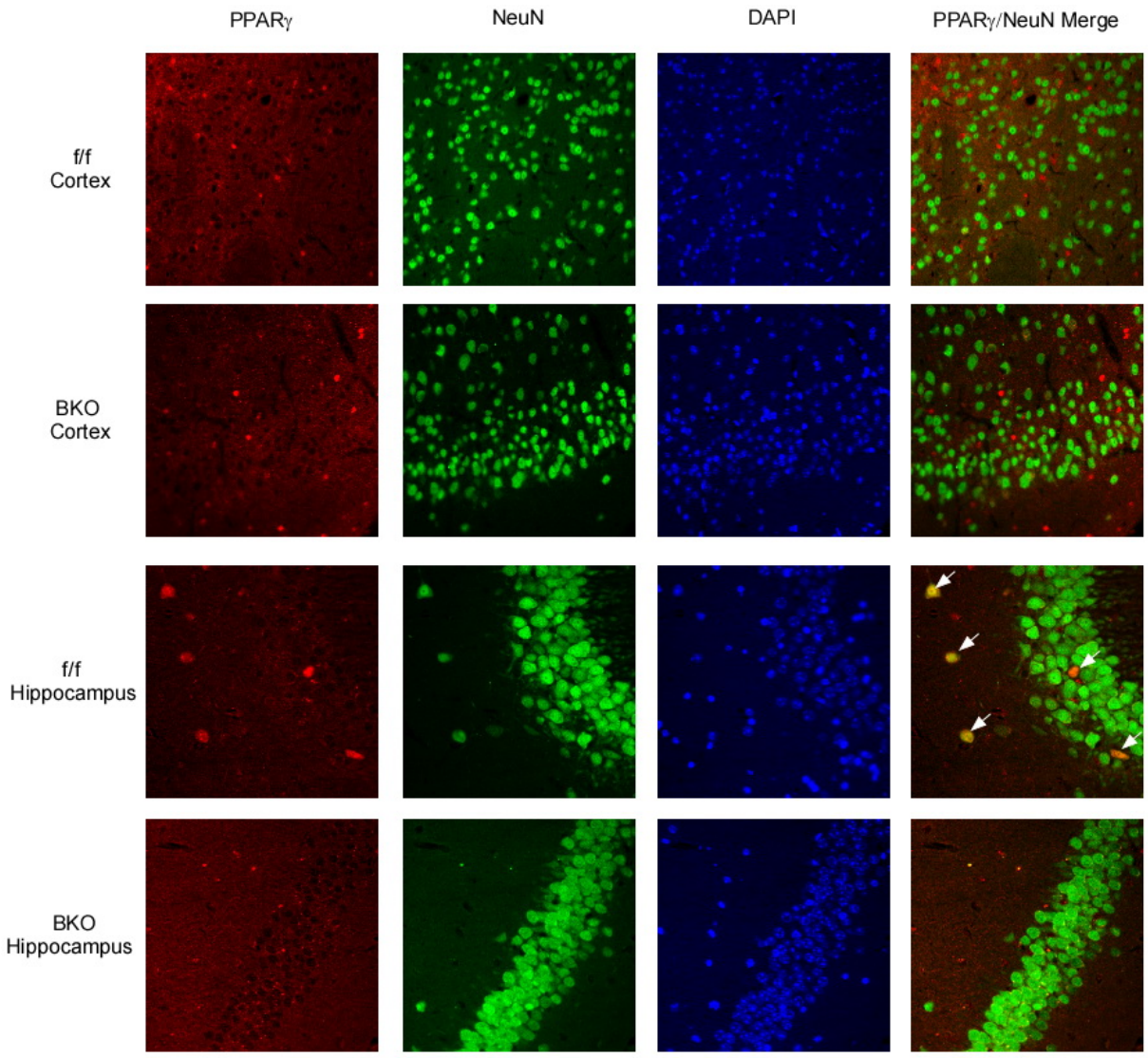

Supplementary Fig. 1. Immunohistochemical (IHC) analysis of coronal brain slices from control and *Pparγ* BKO mice. IHC staining for PPARγ (red), NeuN (green), and DAPI (blue) in coronal brain sections. We used a polyclonal antibody to PPARγ (Cells Signaling Technology, Beverly, MA) and a monoclonal antibody to NeuN (Millipore, Billerica, MA). We used secondary antibodies (Alexa Fluor 488 anti–mouse and Alexa Fluor 546 anti–rabbit) from Invitrogen (Carlsbad, CA). Single color and merged images from cortex and hippocampus of are shown. Arrows indicate $PPAR\gamma^{+}$ $NeuN^{+}$ $DAPI^{+}$ cells.

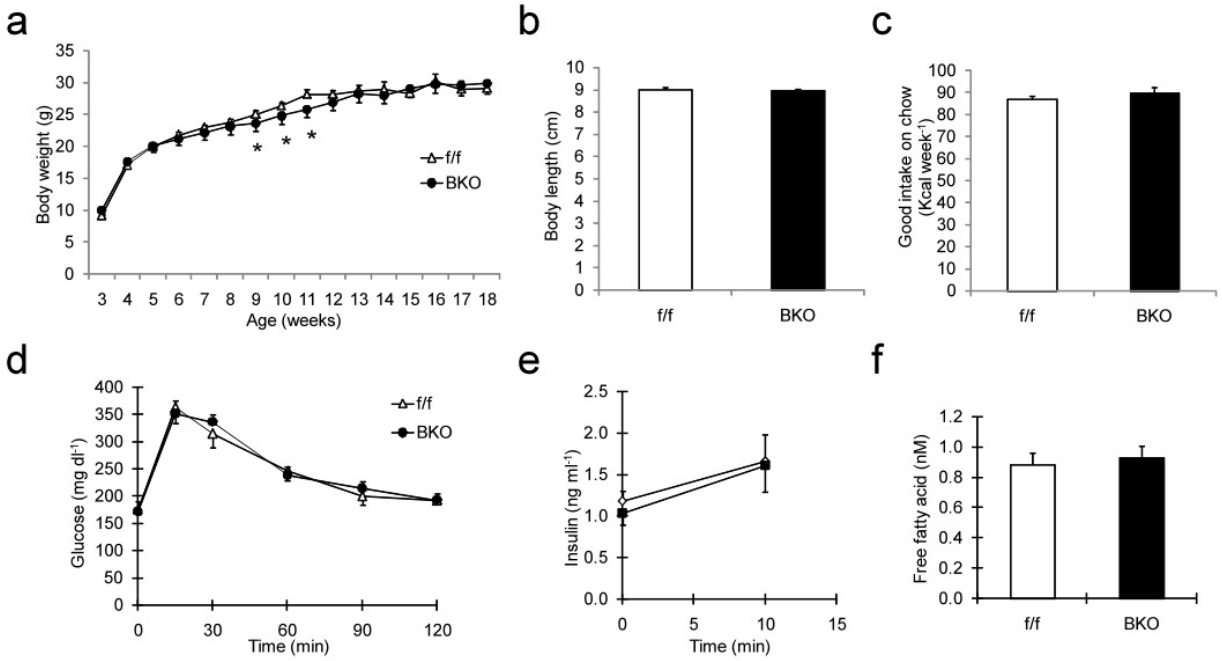

Supplementary Fig. 2. Characterization of control and *Pparγ* BKO mice on chow diet

(**a**) Body weight of *Pparγ* f/f and BKO mice (n = 6–14 per group) fed a standard chow diet from age 3 to 24 wk. (**b**) Body length (anal nasal length) of 6–month old control (n = 9) and BKO mice (n = 8) on chow diet. (**c**) Weekly caloric intake of control (n = 12) and BKO (n = 11) mice fed a standard chow diet. (**d**) IPGTT results from chow–fed control (n = 6) and BKO (n = 6) mice. (**e**) Plasma insulin concentration during IPGTTs in chow–fed control (n = 6) and BKO (n = 6) mice. (**f**) Fasting plasma free fatty acid concentration in chow–fed control (n = 6) and BKO (n = 6) mice. All data are shown as mean ± SEM. Asterisks indicate statistical significance ($p < 0.05$) between control and BKO mice.

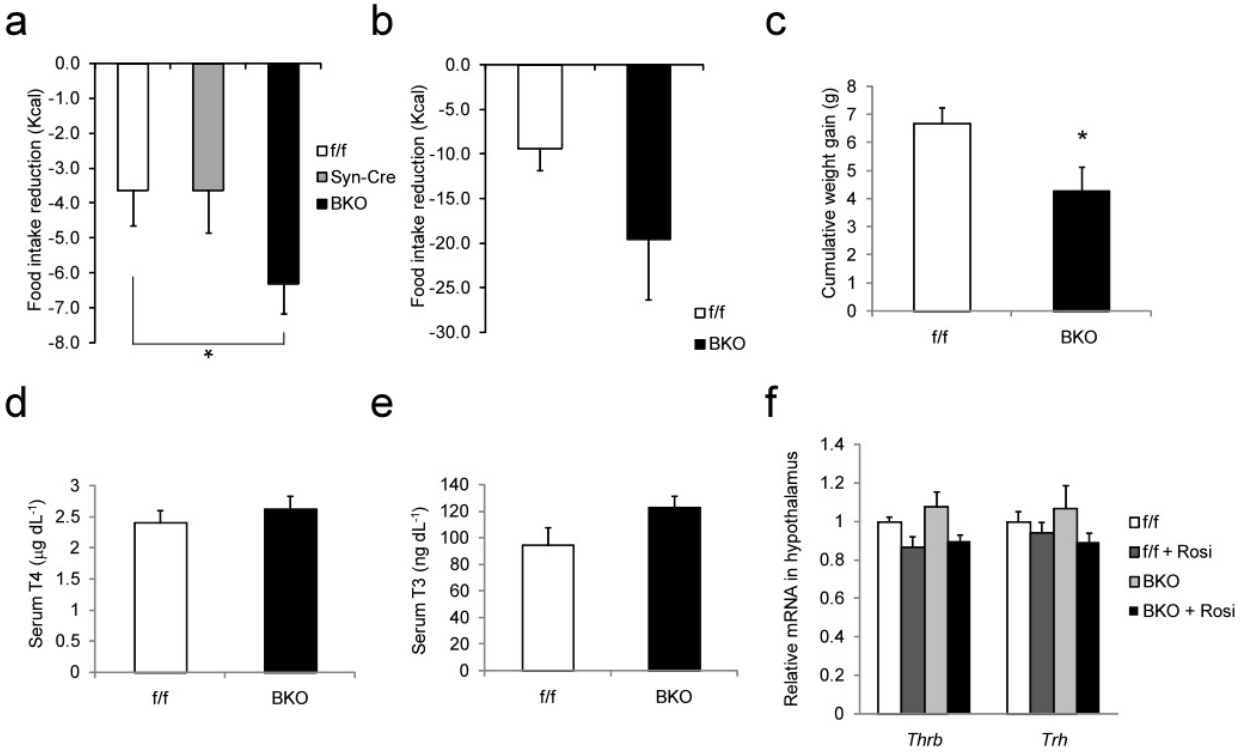

Supplementary Fig. 3. Leptin sensitivity and thyroid function in *Pparγ* BKO mice

(**a**) Leptin sensitivity test in chow–fed *Pparγ* f/f (n = 6), Syn–Cre (n = 8), and *Pparγ* BKO (n = 6) mice. (**b**) Leptin sensitivity test in HFD–fed f/f (n = 8) and BKO (n = 5) mice. Reduction of food intake by twice daily leptin injection (0.5 mg kg^{-1} for chow–fed mice and 1 mg kg^{-1} for HFD mice) in two days is shown as mean ± SEM. (**c**) Cumulative weight gain of 12-wk old f/f and BKO mice (n = 7–9 per group) during 2–wk HFD feeding with rosiglitazone treatment directly switched from chow diet. (**d**) Serum thyroxine (T4) concentration in control (n = 7) and BKO (n = 10) mice. (**e**) Serum triiodothyronine (T3) concentration in control (n = 7) and BKO (n = 10) mice. (**f**) Quantification of hypothalamic thyroid hormone receptor β and thyrotropin–releasing hormone mRNA expression in control and BKO mice (n = 5–8 per group) on HFD with or without rosiglitazone treatment. Data are shown as mean ± SEM. Asterisks indicate statistical significance ($p < 0.05$) between control and BKO mice.

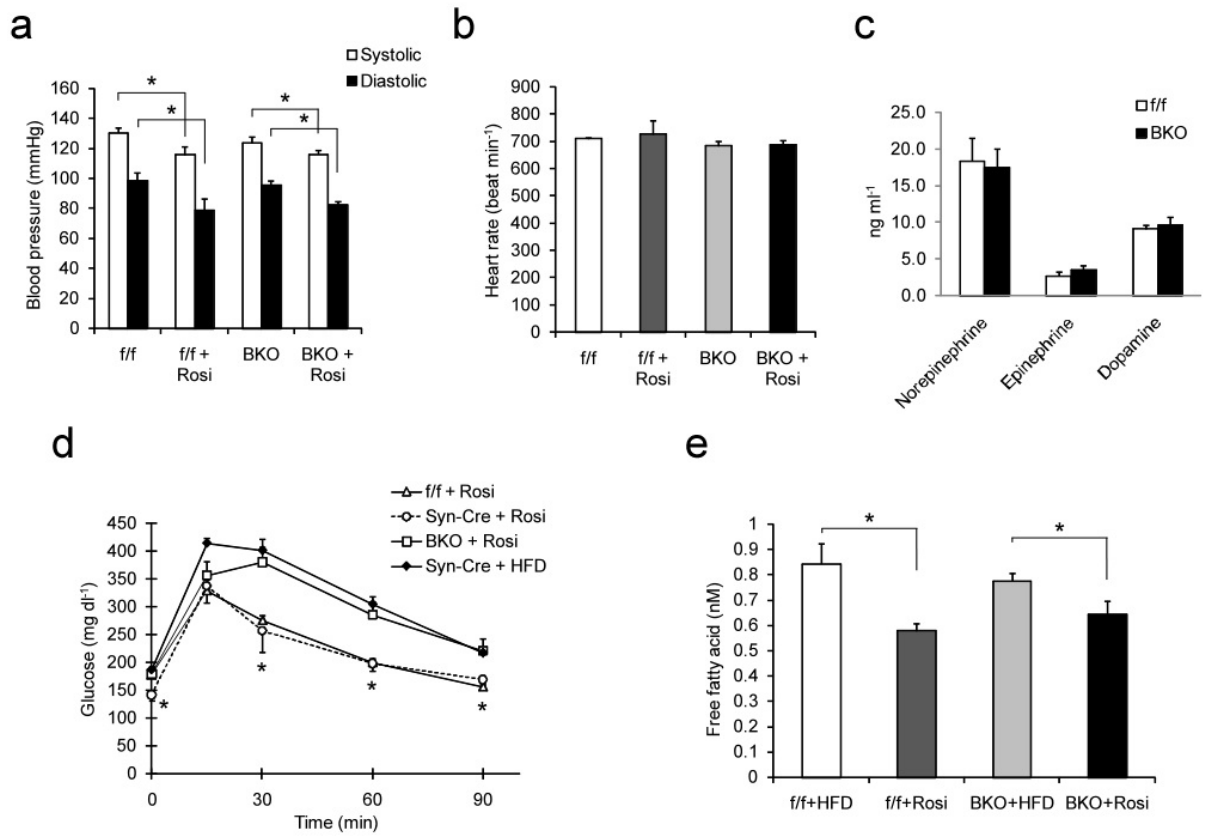

Supplementary Fig. 4. Cardiac parameters and short-term TZD treatment

(**a**) Systolic and diastolic blood pressures of *Pparγ* f/f and *Pparγ* BKO mice on HFD or after rosiglitazone treatment (n = 5–7 per group). (**b**) Heart rate of control and BKO mice on HFD or after rosiglitazone treatment (n = 5–7 per group). (**c**) Serum catecholamine concentrations in rosiglitazone–treated control (n = 7) and BKO (n = 10) mice. (**d**) Intraperitoneal GTTs on *Pparγ* f/f, Syn–Cre, and *Pparγ* BKO mice on HFD or after 3–wk rosiglitazone treatment (n = 4–7 per group). Statistical significance between rosiglitazone–treated Syn–Cre and BKO mice are indicated by asterisks ($p < 0.05$). (**e**) Fasting blood free fatty acid concentration in control and BKO mice on HFD or after rosiglitazone treatment (n = 5–7 per group). All data are shown as mean ± SEM. Except for (**d**), Asterisk indicates statistical significance ($p < 0.05$) between conditions connected by bars.

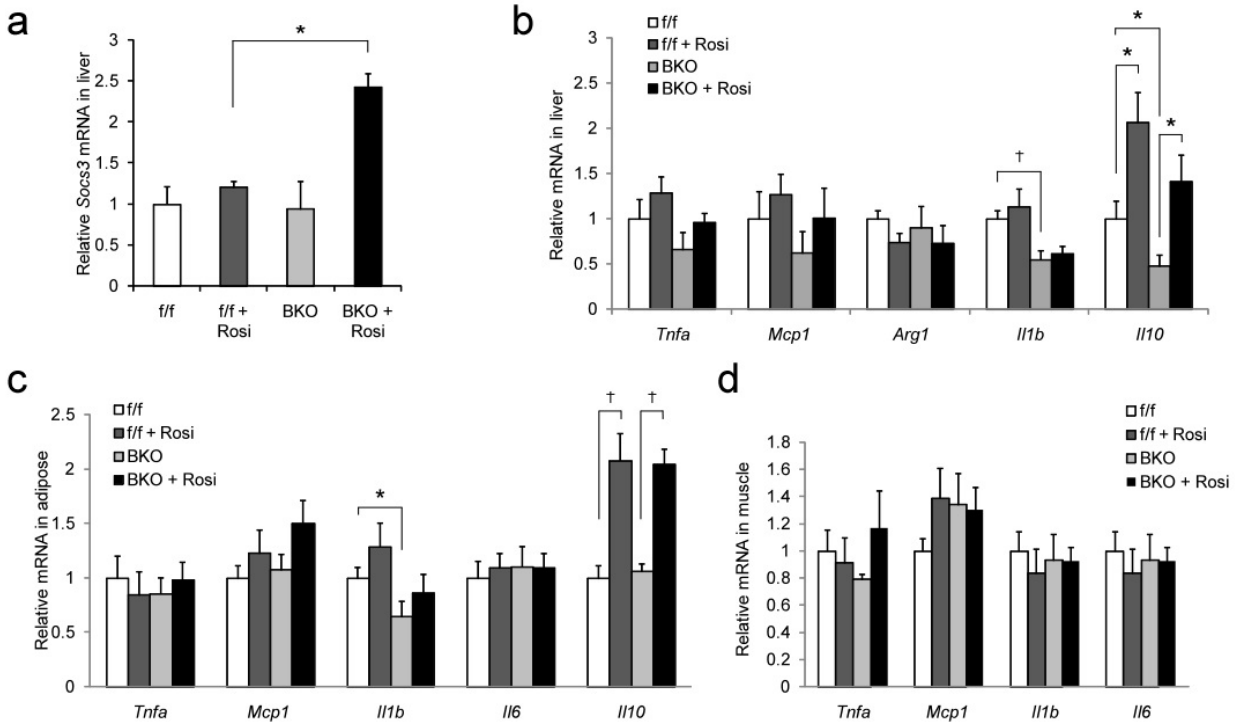

Supplementary Fig. 5. Tissue inflammation in *Pparγ* BKO mice

(**a**) Quantification of *Socs3* mRNA expression in liver of control and *Pparγ* BKO mice on HFD or after rosiglitazone treatment (n = 5–10 per group). (**b**) Measurement of inflammatory gene expression in liver of control and BKO mice on HFD or after rosiglitazone treatment (n = 5–10 per group). (**c**) Measurement of inflammatory gene expression in epididymal WAT of control and BKO mice on HFD or after rosiglitazone treatment (n = 7–15 per group). (**d**) Measurement of inflammatory gene expression in muscle of control and BKO mice on HFD or after rosiglitazone treatment (n = 5–10 per group). All data are shown as mean ± SEM. Statistical significance between conditions connected by bars is indicated by asterisks ($p < 0.05$) or daggers ($p < 0.01$).

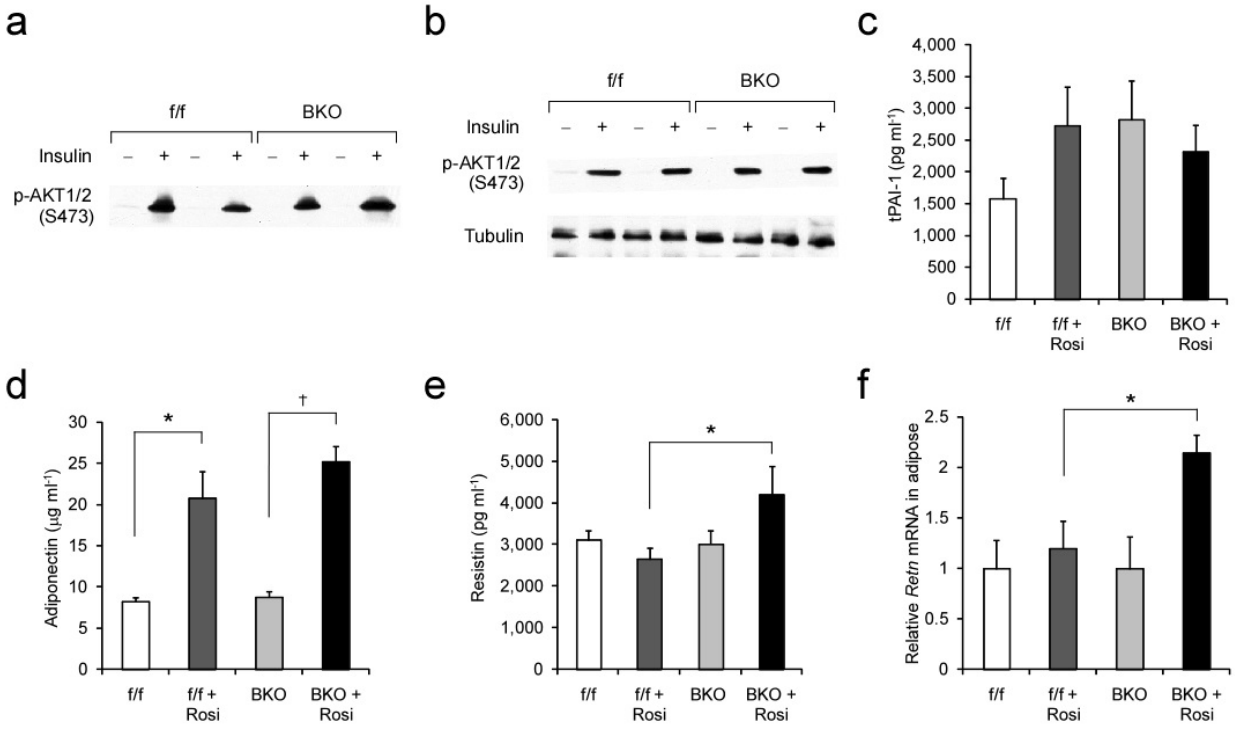

Supplementary Fig. 6. Tissue insulin sensitivity and circulating adipokine concentration

(**a**) Western blot showing acute insulin–stimulated AKT phosphorylation in muscle of rosiglitazone–treated control and *Pparγ* BKO mice. (**b**) Western blot showing acute insulin–stimulated AKT phosphorylation in eWAT of rosiglitazone–treated control and BKO mice. (**c**)–(**e**) Serum adiponectin (**c**), tissue plasminogen activator inhibitor–1 (**d**), and resistin (**e**) concentration in control and BKO mice on HFD or after rosiglitazone treatment (n = 5–8 per group). (**f**) Quantification of *Retn* (resistin) mRNA expression in eWAT of control and BKO mice on HFD or after TZD treatment (n =7–15 per group). All data are shown as mean ± SEM. Asterisk indicates statistical significance ($p < 0.05$) between conditions connected by bars.

Supplemental Table 1. **Multiple regression models for energy expenditure analysis**

Multiple regression models for the effect of genotype (f/f control *vs*. *Pparγ* BKO) on 24–h average energy expenditure in cal min^{-1} adjusted for total body mass and 24–h average activity (Model 1) and for lean body mass, fat mass and 24–h average activity (Model 2). Note that the coefficient estimates for lean body mass and fat mass in model 2 are similar, but that fat mass is the more reliable of the two predictors. Also note that both models identify essentially the same effect of genotype with *Pparγ* BKO mice having a 1 cal min^{-1} higher adjusted metabolic rate compared to control mice. Finally, note that the genotype effect is independent of activity such that differential activity between genotypes does not appear to account for the elevated metabolic phenotype of the KO mice. *Interpretation*: *Pparγ* BKO mice have an elevated metabolic rate phenotype compared to control mice that is not driven by increased activity.

Model	Parameter	Coefficient*	SE	P
1	Intercept	5.642	1.4544	0.0031
$R^2 = 0.63$	Genotype	0.999	0.326	0.0120
	Total body mass (g)	0.214	0.0384	0.0002
	Activity (counts min^{-1})	–0.003	0.0225	0.9053
		I		
	Intercept	5.175	3.5553	0.179
2	Genotype	1.022	0.3129	0.001
$R^2 = 0.68$	Lean body mass (g)	0.25	0.1693	0.175
	Fat mass (g)	0.216	0.0482	0.001
	Activity (counts min^{-1})	–0.001	0.0275	0.98

Change in predicted energy expenditure for each one unit change in the independent variable. Genotype coded 0 = control , 1 = BKO. R^2 = proportion of variance in energy expenditure accounted for by the model.

Supplemental Table 2. Tissue lipid content

	f/f	f/f + Rosi	BKO	BKO + Rosi
LiverTG (mg/gm protein)	1.32±0.13	1.56±0.13	1.53±0.26	1.36±0.28
Liver NEFA (nmol/gm protein)	533.0±26.3	450.3±21.4 *	568.1±50.2	493.7±41.6
Liver DAG (mg/gm protein)	136.8±6.6	110.3±7.7 *	150.1±11.4	123.3±11.4
Liver Ceramide (mg/gm protein)	44.1±5.2	24.8±2.5 *	47.2±4.1	25.2±2.6 #
Muscle TG (mg/gm protein)	6.5±1.2	6.2±0.6	7.2±0.8	6.7±1
Muscle NEFA (nmol/gm protein)	5.2±0.5	6.4±0.5	5.9±0.2	6.2±0.5
Muscle DAG (mg/gm protein)	590±80.5	471.8±51.7	624±118.4	558.3±80.3
Muscle Ceramide (mg/gm protein)	415.7±99.4	219.5±32 *	399±126	231.7±38 #

Data are expressed as mean ± SEM.

Asterisks indicate statistical significance ($p < 0.05$) between f/f and rosiglitazone–treated f/f mice. Ponds indicate statistical significance ($p < 0.05$) between *Pparγ*BKO and rosiglitazone–treated BKO mice.